

A copula-based drought assessment framework considering global simulation models

André S. Ballarin^{a,1}, Gustavo L. Barros^a, Manoel C.M. Cabrera^{b,*}, Edson C. Wendland^{a,2}

^a Department of Hydraulics and Sanitary Engineering, São Carlos School of Engineering (EESC), University of São Paulo (USP), CxP.359, São Carlos, São Paulo 13566-590, Brazil

^b Department of Exact and Technological Sciences, State University of Santa Cruz, Ilhéus, Bahia 45662-900, Brazil

ARTICLE INFO

Keywords:

Meteorological droughts
Multivariate frequency analysis
Global warming
Compound extreme events.

ABSTRACT

Study region: São Paulo state – Brazil.

Study focus: Compound events, such as droughts and heat waves, may have severe impacts on human activities. Traditionally, they are characterized considering a univariate perspective. However, this approach may not be the most adequate to characterize such hazards as they often result from a combination of variables interacting in space and time. Alternatively, several studies adopt the multivariate frequency analysis as it allows the consideration of concurrent drivers and their dependencies. Nevertheless, few of them evaluated this methodology in a climate change context. In view of this, this study aims to compare the uni and multivariate approaches to characterize extreme drought events considering both historical and future scenarios, using the severe water crisis experienced in the southeast region of Brazil in 2014–2015 as a study case.

New hydrological insights for the region: The univariate approach can substantially underestimate the risk associated with extreme events. For future scenarios, differences between the two methodologies reached 90% of the estimated return period. Significant increasing trends were found only for temperature. Both approaches indicated that drought events will be more common and intense in the future. However, the univariate framework may misspecificate the associated risks, as it not account for the expected warming condition that may trigger or exacerbate extreme drought events.

1. Introduction

Hydrological extreme events have received special attention in recent decades due to their increasing impacts in a climate change context (Hao et al., 2018). Despite several scientific advances to characterize them, understanding their mechanisms considering a global warming scenario, where extreme events may happen at increasing rates is still a challenge (Trenberth et al., 2015; Vaghefi et al., 2019). Among various climate extreme events, droughts are by far the most complex and costly natural disaster, representing the

* Corresponding author.

E-mail addresses: andre.ballarin@usp.br (A.S. Ballarin), gbarros703@gmail.com (G.L. Barros), mcmcabrera@uesc.br (M.C.M. Cabrera), ew@sc.usp.br (E.C. Wendland).

¹ ORCID ID: 0000-0001-6997-8662

² ORCID ID: 0000-0003-3374-608X

<https://doi.org/10.1016/j.ejrh.2021.100970>

Received 4 November 2020; Received in revised form 28 October 2021; Accepted 16 November 2021

Available online 22 November 2021

2214-5818/© 2021 The Authors.

Published by Elsevier B.V. This is an open access article under the CC BY license

(<http://creativecommons.org/licenses/by/4.0/>).

main natural cause of socioeconomic and environmental damage across the globe (Hao et al., 2014; Pendergrass et al., 2020; Pulwarty and Sivakumar, 2014; Vicente-Serrano et al., 2014). To avoid their potential consequences, a reliable characterization process is required to provide substantial knowledge for improving risk assessment and decision-making.

Conventionally, drought events are characterized considering one single and representative variable in a univariate framework (e.g. precipitation anomalies through the standardized precipitation index (SPI) to characterize meteorological droughts) (AghaKouchak et al., 2014; Coelho et al., 2016a; Mesbahzadeh et al., 2020; Sheffield and Wood, 2008). However, drought events may be triggered or exacerbated by a combination of concurrent variables interacting in space and time, such as precipitation anomaly and high temperature as observed in several recent events (AghaKouchak et al., 2014). Therefore, to improve drought analysis, it is important to consider its multivariate characteristic, assessing all important variables involved in the process (Leonard et al., 2014; Mesbahzadeh et al., 2020; Salvadori and De Michele, 2004; Serinaldi, 2016).

Several studies have applied multivariate frequency analysis, such as copula functions, to overcome limitations in the characterization of extreme drought events (AghaKouchak et al., 2014; Fischer and Knutti, 2013; Gräler et al., 2013; Masud et al., 2015; Serinaldi, 2016; Zscheischler and Seneviratne, 2017). This approach provides a great potential to characterize compound events as it allows risk assessment of different variables considering their dependence structure. However, in these studies, little attention has been paid to the characterization of extreme events considering future scenarios (Mechler and Bouwer, 2015). Droughts may intensify in the future in many regions of the world as a consequence of increasing atmospheric evaporative demand caused by the increase in global temperatures (Pendergrass et al., 2020; Vicente-Serrano et al., 2014; Wang et al., 2012). Compound intensification in both precipitation deficit and temperature extremes may exacerbate their impacts. Furthermore, two non-extreme conditions combined may result in an extreme condition with significant impacts (AghaKouchak et al., 2014; Leonard et al., 2014). In this context, an accurate characterization of droughts considering future scenarios in a multivariate framework may help risk assessment practices and prevent future damage (Melo and Wendland, 2017; Mesbahzadeh et al., 2020).

In the present study, we evaluated two different approaches (uni and multivariate) to risk assessment of extreme droughts events considering both historical and future conditions. Using temperature and precipitation data, we characterized the severe water crisis experienced in São Paulo state, located in the southeast region of Brazil, between 2014 and 2015 (Marengo et al., 2018; Nobre et al., 2016), which impacted about 11 million people in Brazil's most populated region (Coelho et al., 2016b; Getirana, 2016; Melo and Wendland, 2016; Nobre et al., 2016). By using this extreme drought event as a study case, we aimed: (i) to identify the influence of the joint occurrence of precipitation-temperature extremes on the characterization of drought events; and (ii) to evaluate relative changes in future droughts compared with the historical period considering both uni and multivariate frameworks. Given the multivariate characteristic of droughts, we argue that the copula approach can improve the understanding of these events, helping decision-makers to optimize drought management practices, considering that drought impacts may be exacerbated by an intensification in temperature (Vicente-Serrano et al., 2014).

2. Material and methods

2.1. Study area and the 2014–2015 drought

The study focuses on the most populated state of Brazil, São Paulo, located between 26–19°S and 54–46°W. The region is characterized by a wet period in the austral summer, which starts in December and ends in February (Obregón et al., 2014), and a dry winter, from June to August (Dufek and Ambrizzi, 2008). On the other seasons (autumn and spring), the region presents intermediate conditions of precipitation (Coelho et al., 2016a). However, the region is sensitive to climate anomalies. The rainfall variability in the region, from daily to decadal timescales, is affected by different sources, such as the South Atlantic Convergence Zone (SACZ), which is the main mechanism responsible for rainfall in the summer season (Otto et al., 2015), frontal systems and the humidity flux from Amazonia (Coelho et al., 2016b; Dufek and Ambrizzi, 2008; Obregón et al., 2014). Some other studies also evaluated the effects of El Niño Southern Oscillation (ENSO) on rainfall in São Paulo, showing that it may affect the inter annual variability, despite its complex and not well defined signal (Coelho et al., 2002; Kane, 2000; Obregón et al., 2014).

The state experienced a major drought in 2014–2015, which resulted in several impacts related to water availability for human consumption, hydropower production and agricultural irrigation (Coelho et al., 2016b). The main water supply system of the Brazilian megacity of São Paulo (Cantareira system) dropped below 15% of its capacity, affecting about 11 million people (Melo et al., 2016; Seth et al., 2015). According to Nobre et al. (2016), the complexity and severity of the observed drought resulted from a mix of abnormal amounts of precipitation, extreme high temperatures and from the high vulnerability of the supply systems.

The atmospheric condition in the region blocked the passage of cold fronts from the south and the flux moisture from the Amazon region, culminating in a extreme dry condition (Coelho et al., 2016b; Seth et al., 2015). Extreme high temperatures affected the water availability, increasing the water consumption, evapotranspiration and the soil moisture deficiency. Moreover, other major factor that aggravated the water crisis is related to changes in the water use. São Paulo's population grew approximately 20% in the past 20 years, impacting directly the water consumption (Otto et al., 2015). So, while precipitation deficits reduced water availability and high temperatures increased the water consumption, the rapid development and expansion of the population in São Paulo state increased the exposure and vulnerability of supply systems (Coelho et al., 2016b, 2016a; Nobre et al., 2016; Otto et al., 2015).

2.2. Characterization of drought events

Drought events can be defined in multiple ways and be influenced by multiple drivers (Otto et al., 2015). Their different concepts

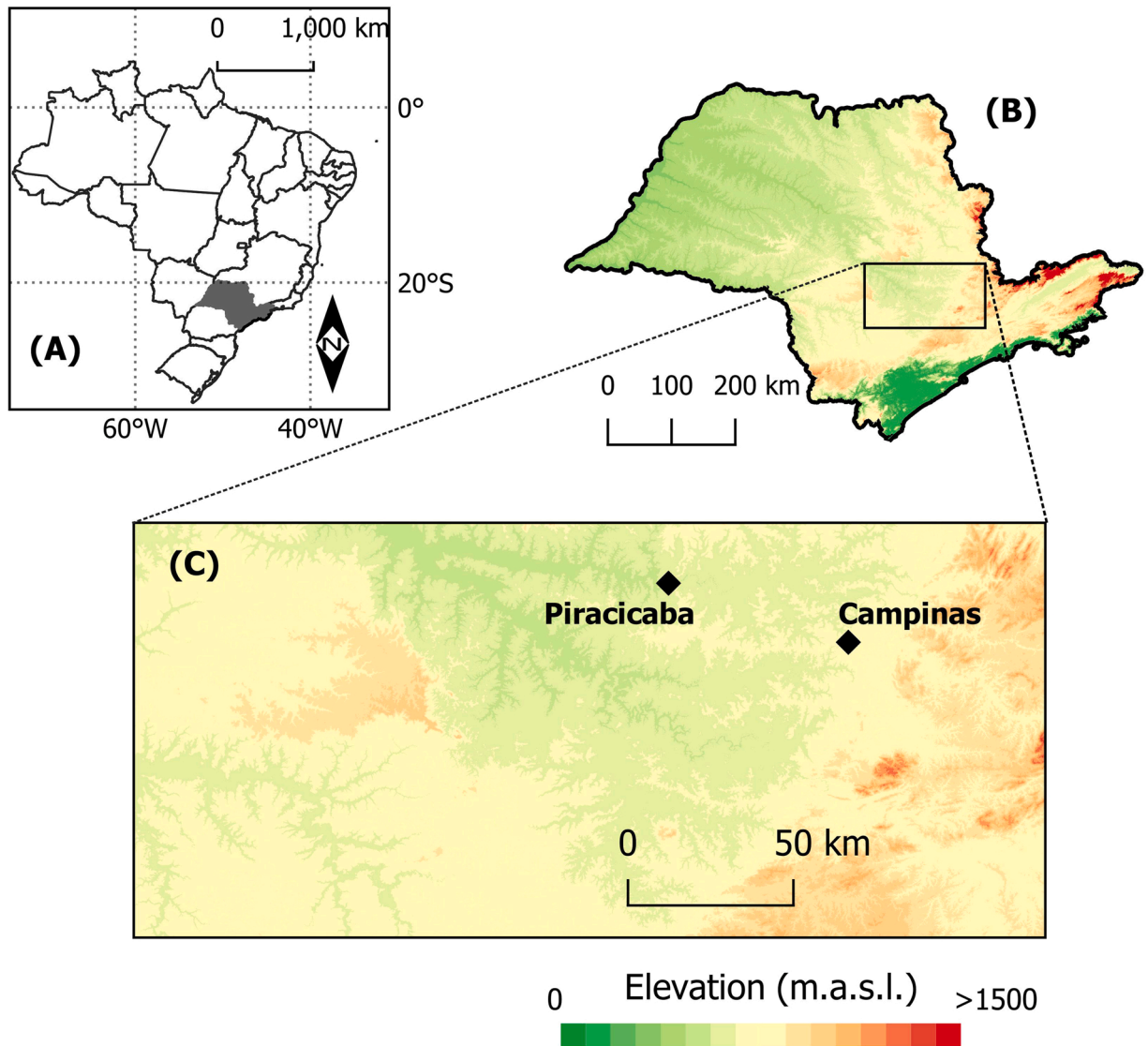


Fig. 1. (A) São Paulo state (highlighted in gray) in the national context. (B) Elevation map of São Paulo state. (C) Location of the two meteorological stations (Campinas - IAC and Piracicaba - ESALQ) considered in the context of our study area.

and uses may vary according to the aim of the study (Melo and Wendland, 2016). In this paper, we focused on meteorological droughts, which are popularly defined as a period of deficits in precipitation (Kao and Govindaraju, 2010; Wilhite and Glantz, 1985). However, considering the possible multivariate aspect of droughts, we also opted to evaluate them through an alternative perspective, considering the joint occurrence of extreme hydroclimatic events: meteorological droughts (precipitation deficit) and high temperatures (heat waves), which is the worst case from a socioeconomic point of view. This approach is particularly relevant to the study region and may apply to other tropical environments, since the simultaneous occurrence of high temperatures and precipitation deficits may trigger or exacerbate water supply hazards (Vicente-Serrano et al., 2014). Moreover, extreme temperature is projected to increase in the region according to climate change scenarios. This condition may substantially increase the chance of concurrent precipitation deficits and heat waves (Aghakouchak et al., 2014).

In Brazil, 83% of the produced energy is renewable. Hydroelectricity represents 64% of the total energy matrix. In this context, a severe precipitation deficit reduces the electricity production due to smaller volume of stored water and lower hydraulic head. On the other hand, heat waves increase evaporation, human water consumption and agriculture irrigation further reducing the water availability in storage dams. In addition, the energy demand for public water supply, air conditioning and food preservation increases. Therefore, the consideration of precipitation and temperature as compound events aims to account for these possible issues.

2.3. Precipitation and temperature data

2.3.1. Observed data

In contrast to [AghaKouchak et al. \(2014\)](#) and [Serinaldi \(2016\)](#), who used aggregated data (temperature and precipitation) of the rainy season to characterize the 2014-California severe drought, we aggregated the precipitation and rainfall data considering the entire year. Such as [Filho et al. \(2020\)](#) and [Melo et al. \(2016\)](#), we opted for this time scale as it is the time required for the effects of droughts to be felt on different sectors, such as agricultural activities, water resources management and hydropower production. By doing this, we included the effects of high temperatures and abnormal amounts of precipitation that occurred in the dry season (approximately 20% of the annual volume), which also affected the water supply system of the region in the severe 2014-water crisis by increasing water consumption and the soil moisture deficiency, as showed by [Nobre et al., \(2016\)](#), [Coelho et al. \(2016b\)](#) and [Melo et al. \(2016\)](#).

Moreover, the consideration of this temporal scale allowed us to ensure consistency with the analysis of future scenarios. As shown by [Almazroui et al., \(2021\)](#), future projections indicate a shift in seasonality and intra-annual variability of precipitation events in Brazil. Historically drier months will increase their contribution to the annual total, while rainier months will have a decrease in their contribution. That is, the definition of dry and rainy seasons may vary throughout the future projections. Therefore, the consideration of the annual scale allowed us to avoid the possible problem of incorrectly defining the rainy and dry seasons in future scenarios.

We considered data of two rain gauges with centenary rainfall-temperature records. The datasets were obtained from the Agromic Institute of Campinas (IAC) and the Luiz de Queiroz College of Agriculture (ESALQ) in Campinas and Piracicaba, respectively, which are cities located in São Paulo state ([Fig. 1](#)). Although the data were previously quality checked, we eliminated some inconsistent data, such as those with an incorrect order of magnitude. The missing values in both series were filled according to the correlation method ([Sattari et al., 2017](#)), using data from three auxiliary stations. Some statistical properties of the two evaluated series can be seen in the [Supplementary Material \(Table S1\)](#).

2.3.2. Future simulation

The projected rainfall and temperature datasets used to characterize future conditions are available at PROJETA ('Climate Change Projections for South America regionalized by the Eta Model'), from the National Institute for Space Research (INPE). These data were generated using the INPE's RCM, the Eta model for South-America, which downscales the projections of two different global climate models (GCM): MIROC5, and the HadGEM2-ES, which was used in this study due to its higher resolution in PROJETA's downscaling products.

The dynamic downscaling method used in RCMs can capture the global climate simulations generated by GCMs for smaller grid sizes, considering local features and dynamics to improve the resolution of the simulations used in local studies ([Chou et al., 2014a](#); [Chou et al., 2014b](#)). For the southeastern region of Brazil, where Sao Paulo state is located, the model presents a 5 km spatial resolution. The future simulations available on PROJETA consider the future scenarios established in the IPCC 5th Assessment Report (AR5), the so-called RCPs (Representative Concentration Pathway scenarios), which are based on different concentrations of greenhouse gases, expressed in terms of global radiative forcing in 2100 ([Lyra et al., 2018](#)).

We considered two different RCPs in this study. The first, RCP4.5, represents an intermediate scenario, predicting a 4.5 W.m⁻² global forcing radiation at the end of the twenty-first century, assuming a reduction in emissions over the years through the application of climate policies and clean technologies ([Almagro et al., 2017](#)). The second, RCP8.5, assumes an 8.5 W.m⁻² global forcing radiation in 2100, representing the most pessimistic scenario, in which there are no climate policies, resulting in intensifying emissions and use of fossil fuels.

Although RCMs improve the resolution of GCMs, they may suffer from systematic errors in their simulations - resulting from the used GCM and/or the downscaling procedure - which are systematically propagated throughout their future projections ([Kotlarski et al., 2014](#); [Liang et al., 2008](#)). In a recent study, [Almagro et al. \(2020\)](#) indicated that INPE's Eta RCM had systematic errors in rainfall simulations in both downscaled GCM simulations (HadGEM2-ES and MIROC5), suggesting that both products need a bias correction procedure to overcome these limitations and to guarantee more reliable future projections, as it is expected that these biases are also propagated in RCP4.5 and RCP8.5 scenarios.

To deal with these systematic errors, we applied the quantile delta mapping (QDM), proposed by [Cannon et al. \(2015\)](#) - (see [Figs. S2 and S3](#) for details about its performance compared with the simulated series of INPE's Eta RCM). This methodology corrects systematic biases of modeled and observed series, preserving the relative changes between future and historical simulated quantiles. Its algorithm follows three steps. First, we fit a probability distribution to the observed and simulated (historical and future) series, associating quantiles to a non-exceedance probability. After that, a relative change factor (Δ) is defined for these quantiles, associating simulated values of historical and future periods ([Eq. 2](#)). Finally, following the quantile mapping technique, future bias-correction projections are obtained by multiplying the historical simulated values (bias-corrected using the observed values) by the relative factor ([Eq. 3](#)). [Eqs. \(2 and 3\)](#) are relative to the multiplicative expression, suitable for precipitation variables. For temperature variables, we use the additive expression (see Appendix A in [Cannon et al. \(2015\)](#)).

$$\Delta(t) = \frac{Q_{f,s}(t)}{F_{h,s}^{-1}(F_{f,s}(Q_{f,s}(t)))} \quad (1)$$

$$Q_c(t) = F_{h,o}^{-1}(F_{f,s}(Q_{f,s}(t))) \times \Delta(t) \quad (2)$$

where $Q_{f,s}(t)$, $F_{f,s}$, $F_{h,s}^{-1}$ are the t th quantile of the future data, the cumulative distribution function (CDF) fitted to future data and the inverse CDF corresponding to the simulated data during the historical period, respectively. In Eq. (3), $F_{h,o}^{-1}$ is the inverse CDF fitted to historical observed data and $Q_c(t)$ the bias-corrected t th quantile of projections, given the relative change between historical and future data and the bias-corrected historical value.

2.4. Trend estimation

In order to verify the presence of statistical significant trends in the observed and simulated series, we applied the non-parametric rank-based Mann-Kendall test (MK). If a significant trend was found, its magnitude was computed using the Theil-Sen slope estimator (TS). The MK test is the most popular statistical test for trend detection in hydrological studies (Villarini et al., 2009). To address serial autocorrelation issues, we adopted the modified MK test, proposed by Hamed and Rao (1998), in this work. This methodology suggests a variance correction to improve the trend detection. Similar to the MK test, the TS estimator is a robust non-parametric statistic, widely applied in hydrological studies, which shows little influence regarding the presence of outliers (Chagas and Chaffe, 2018; Yue and Hashino, 2007).

2.5. Design value – univariate framework

We evaluated the suitability of six probability distribution functions (pdf) widely used in hydrological frequency analysis to model precipitation and temperature anomalies (Gumbel - GUM, Generalized Extreme Value - GEV, Pearson III – PE3, Generalized Normal - GNO, Generalized Logistic - GLO, and Weibull – WEI). Their parameters were estimated based on the L-Moments method, which has many advantages over other popular estimation methods, such as its ability to characterize a wider range of distribution and its robustness for short samples (Ahmad et al., 2016; Hosking, 1990; Salinas et al., 2014). We used Weibull's plotting position to estimate the non-exceedance probability of the observed series.

The best probability distribution was selected based on their performance in three popular goodness-of-fit-criteria: Root Mean Square Error (RMSE), Akaike Information Criterion (AIC) and Nash-Sutcliffe efficiency (NSE). The RMSE focuses on minimizing the error residuals between the observed and estimated values, selecting the model with the lowest RMSE value. The AIC is based not only on minimizing the residuals, but also on the complexity of the model (degrees of freedom expressed by the number of parameters of the model). Lower values of AIC represent better models. The NSE, introduced by Nash and Sutcliffe (1970), compares the performance of the model with regards to a naïve forecast, considered as the average of the observations. NSE values close to 1 indicate better models (Gupta et al., 2009; Jackson et al., 2019). We also visually assessed the suitability of the probability distributions through a quantile-quantile (Q-Q) plot.

Finally, from the performance of each evaluated probability distribution on RMSE, AIC and NSE, we selected the best probability distribution, which best describes the statistical properties of the observed series. The selected pdf was then used to define design values of the analyzed variables, relating quantiles with specific return periods.

2.6. Design value – multivariate framework

The multivariate approach was conducted using copula functions as it can couple two or more observed variables, describing their dependence well (Salvadori and De Michele, 2004). We considered both variables involved in the study – precipitation and temperature – as X and Y , respectively and denoted F_X and F_Y as their cumulative distribution functions, and $F_{XY}(x, y) = P(X \leq x, Y \leq y)$ as the joint distribution function. If F_X and F_Y are continuous, there is a copula function C , unique, which can be used to obtain $F_{XY}(x, y)$:

$$F_{XY}(x, y) = C(F_X(x), F_Y(y)) \quad (3)$$

For each realization of X and Y , there is a unique isoline (or critical layer) on which both variables share the same probability $t \in (0, 1)$. This critical layer, associated with probability t , defines three regions: the critical region, where $F_{XY} < t$; the alert region, with $F_{XY} = t$ and the safe one, where $F_{XY} > t$ (Salvadori et al., 2013). Eq. 5 defines the return period of the compound event in a multivariate approach, whose analysis complies with the idea of the univariate return period.

$$T_{KEN} = \frac{\mu}{1 - K(t)} \quad (4)$$

where μ is the time between subsequent values of the observed variables in the time series, i.e., the average interval time between X_i and X_{i+1} (or Y_i and Y_{i+1}); T_{KEN} is the Kendall's return period, introduced by Salvadori et al. (2011), and $K(t)$ is the Kendall's distribution function associated with copula C (Eq. 6). The return period κ_{xy} is clearly a function of the critical layer associated with probability t .

$$K(t) = P(C(F_X(x), F_Y(y)) \leq t) \quad (5)$$

In a multivariate framework, we have a multiple choice to define the critical region, as the variables can combine in different ways (Serinaldi, 2016). Different scenarios can be used to describe the extreme event, leading to distinct critical regions (Salvadori et al., 2016; Serinaldi, 2015, 2016). In this study, we opted for the Kendall's scenario formulation (described above), which defines a unique

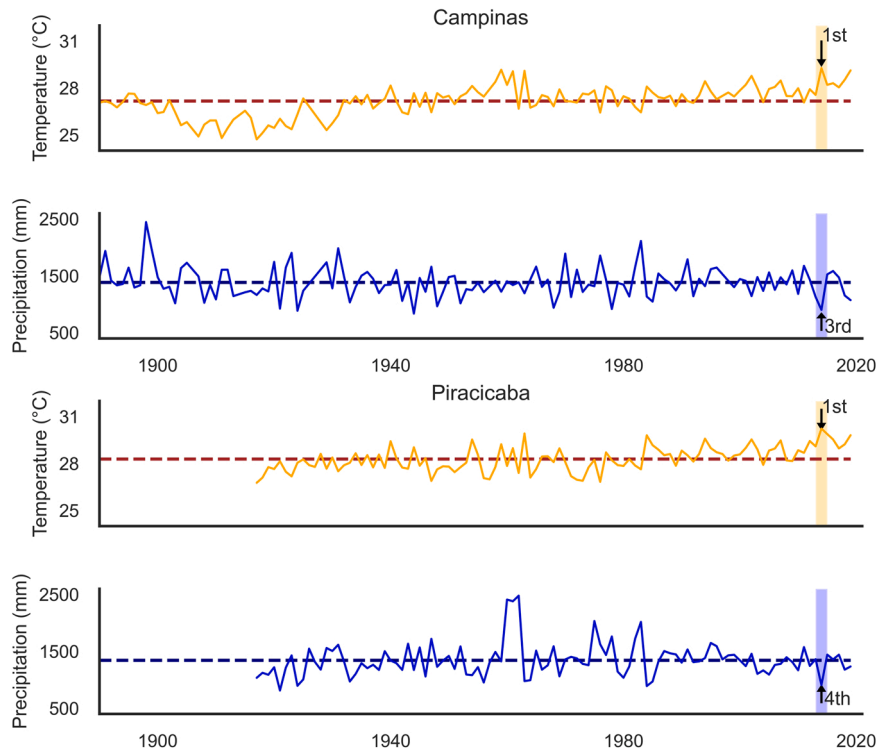


Fig. 2. Temperature (orange line) and Precipitation (blue line) historical series of IAC (Campinas) and ESALQ (Piracicaba) stations. Dashed lines express the mean values of the series. The 2014–2015 drought in the study region is highlighted in the graph, as well as its position in the rank of extreme events. (For interpretation of the references to color in this figure legend, the reader is referred to the web version of this article.)

dangerous region for all events lying over a critical layer (Salvadori et al., 2011). In other words, the uses of Kendall’s approach ensures that all events with larger return periods of the design value are in the dangerous region (Gräler et al., 2013).

Alternatively, the “AND” scenario (Eq. 7), described in Salvadori et al. (2016), was also analyzed to evaluate design quantiles and return periods from another perspective. Unlike the Kendall scenario whose definition is based on the identification of a critical layer, in this scenario, the return period is based on both variables that exceed a certain threshold (Mesbahzadeh et al., 2020). We opted not to use the “OR” scenario considering that drought events are triggered by extreme conditions in both precipitation and temperature, not only in one of them. Moreover, as pointed out by Salvadori et al. (2016), the Kendall scenario represents the intersection of infinite “OR” scenarios lying over a specific critical level that identifies the dangerous region. Thus, when using Kendall’s scenario, we are indirectly considering all the dangerous realizations that characterize the “OR” scenario from a summarized perspective.

$$P_{AND} = P(X > x \cap Y > y) = 1 - F_X(x) - F_Y(y) + C(F_X(x), F_Y(y)) \quad (6)$$

$$T_{AND} = \frac{\mu}{P_{AND}} \quad (7)$$

There are different copulas used in multivariate meteorological and hydrological analysis (Gräler et al., 2013; Kao and Govindaraju, 2010, 2007; Kwon and Lall, 2016; Sadegh et al., 2018, 2017; Salvadori et al., 2013; Salvadori and De Michele, 2004; Serinaldi et al., 2009; Sun et al., 2019). In this work, using the MvCAT toolbox, developed by Sadegh et al. (2017), 26 different copulas (Gaussian, t, Clayton, Frank, Gumbel, Independence, Ali-Mikhail-Haq, Joe, Farlie-Gumbel-Morgenstern, Gumbel-Barnett, Plackett, Cuadras-Auge, Raftery, Shih-Louis, Linear-Spearman, Cubic, Burr, Nelsen, Galambos, Marshall-Olkin, Fischer-Hinzmann, Roch-Alegre, Fischer-Kock, BB1, BB5 and Tawn) were analyzed to characterize the meteorological drought events. This tool uses the Markov Chain Monte Carlo (MCMC) simulation, in a Bayesian framework, to estimate copula parameters and their uncertainties. This method ‘converts’ the posterior distribution of the parameter values into uncertainty intervals for the probability isolines.

As highlighted by Sadegh et al. (2017), the correct choice of the copula functions may greatly affect the characterization process, as the copula functions may differ significantly. The toolbox ranks the performance of the copulas based on several goodness of fit criteria: the Maximum Likelihood (ML) value, Bayesian Information Criterion (BIC) and Akaike Information Criterion (AIC), Root Mean Square Error (RMSE) and Nash-Sutcliffe Efficiency (NSE). The best copula function is the one with the best performance in these tests. As well as RMSE and NSE, ML is based only on the minimization of error residuals between estimated and observed values. On the other hand, BIC takes into account the model complexity, such as AIC. In this study, we transformed the precipitation and temperature data to an anomaly perspective, as suggested by AghaKouchak et al., (2014) and Serinaldi (2016).

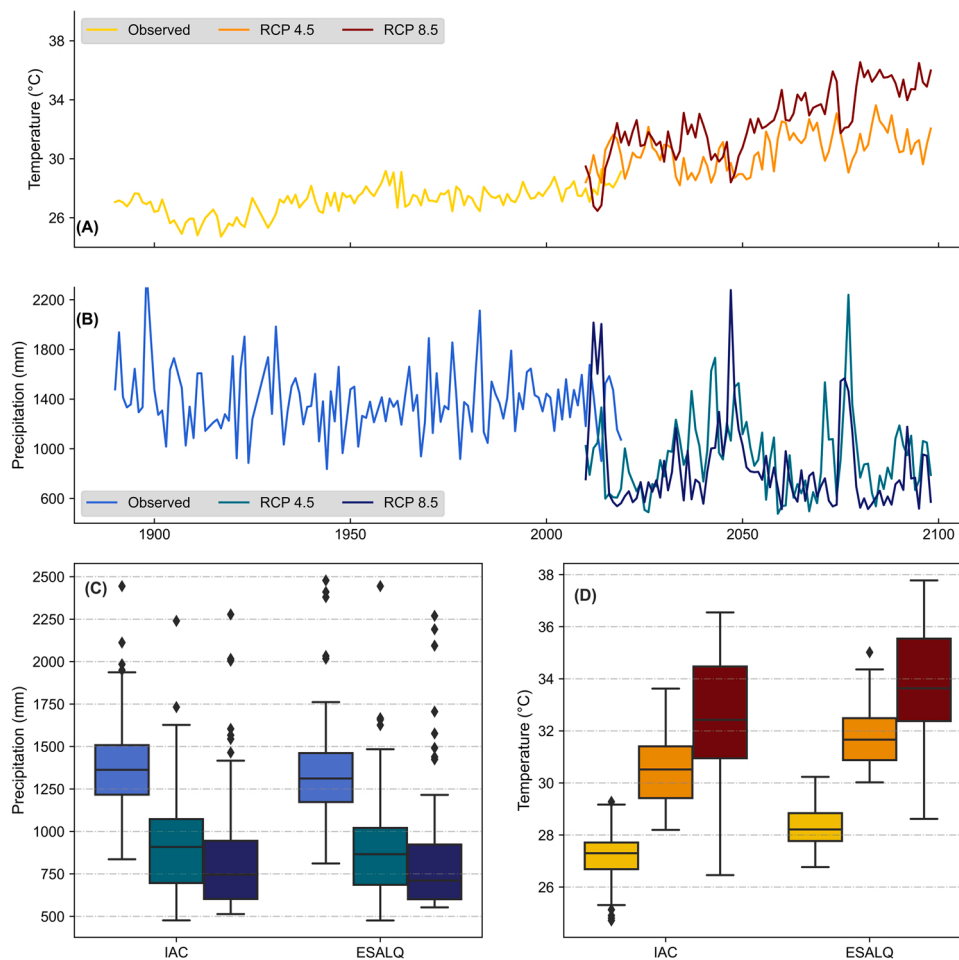


Fig. 3. Temperature (A) and precipitation (B) series of Campinas for the observed period and future scenarios (RCP 4.5 and RCP 8.5). Boxplot showing precipitation (C) and temperature (D) data for Campinas (IAC) and Piracicaba (ESALQ). The colors of the boxes in Figs. C and D share the same legend as Figs. A and B. (For interpretation of the references to color in this figure legend, the reader is referred to the web version of this article.)

3. Results and discussion

3.1. Temperature and precipitation series

3.1.1. Observed data

Although the 2014–2015 drought in the study region experienced a dry condition, the region had already seen worse situations related to precipitation deficits. If we consider the annual precipitation in Campinas in 2014 (900.9 mm), it can be seen that it is not the most extreme situation, representing only the third position in the ranking of dry years (Fig. 2). Considering the recorded period (1890–2019), drier situations can be observed in 1944 (836.5 mm) and 1924 (886.2 mm). The same happens with Piracicaba, where the 2014 total annual precipitation (906 mm) represents the fourth position in the dry condition ranking. The driest conditions can be seen in 1921, 1984 and 1924, with 812 mm, 890 mm, and 894 mm, respectively.

However, according to the historical series of Campinas, the warmest condition was observed in 2014 with a maximum temperature of 29.28 °C (Fig. 2). This condition made the 2014–2015 drought unique, having several economic and social impacts. In comparison, the average daily maximum temperature at the driest year (1944) was only in the 35th position of the warmest year. Thus, even though 1944 experienced the driest condition, it not experienced an extreme drought condition with water supply impacts, as what happened in 2014–2015. In fact, the region already experienced similar dry conditions historically, however none of them resulted in an extreme drought such as in 2014 (Coelho et al., 2016b). The same happens with the Piracicaba, where the driest year (1921, with annual rainfall of 812 mm) occupies only the 48th position in the ranking of the warmest years. Again, no water crisis was registered in this year, even with the driest condition.

Table 1

Selected univariate probability distributions for temperature and precipitation series of Campinas and Piracicaba.

Series	Criteria	Best Distribution	Selected Distribution
Piracicaba - Precipitation	NSE	GEV	GLO
	AICc	GLO	
	RMSE	GLO	
Piracicaba - Temperature	NSE	GEV	GEV
	AICc	GLO	
	RMSE	GEV	
Campinas - Precipitation	NSE	GLO	GLO
	AICc	GLO	
	RMSE	GLO	
Campinas - Temperature	NSE	GLO	GLO
	AICc	GLO	
	RMSE	PE3	

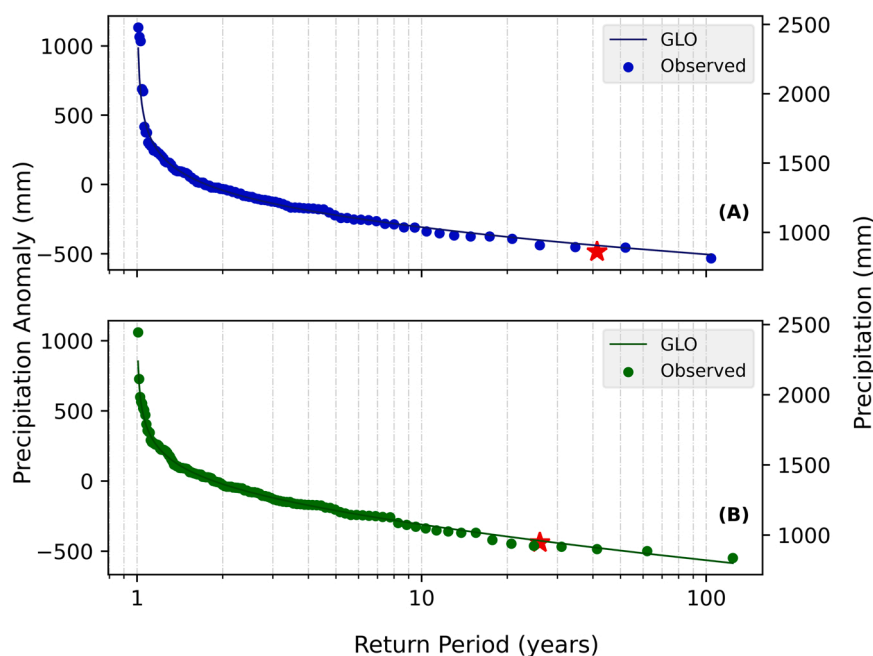


Fig. 4. Return period for both stations in the univariate framework. (A) Piracicaba (B) Campinas. The annual observed precipitation, concerning the 2014–2015 drought in the study region, is shown in red. (For interpretation of the references to color in this figure legend, the reader is referred to the web version of this article.)

3.1.2. Future data

Both future scenarios considered in this study showed an intensification in meteorological droughts, expressed by a drier and warmer climate, highlighting the relative changes in both precipitation and temperature (Fig. 3). As expected, the pessimistic scenario (RCP 8.5) presents worse drought conditions, with higher and lower values of average daily maximum temperature and annual precipitation, respectively, when compared with the intermediate scenario (RCP 4.5). Considering both future scenarios, an increase in the maximum temperature range is expected (from +3.5 to +5.5 °C, approximately). Even if no changes were expected in the annual precipitation, the maximum temperature intensification would lead to an increase in drought severity (AghaKouchak et al., 2014). The boxes in Fig. 3c and d confirm the high uncertainty level expected for future scenarios. However, the changes in both scenarios and stations (Campinas and Piracicaba), corroborate the idea that drought events in the future will be more common and intense compared with the dry occurrences observed now.

3.2. Trend Estimation

The results of the MK test, applied to the dataset, show that all temperature series (observed and future periods) present significant trends at a 5% significance level. However, for precipitation series, no significant trends were found. Analyzing the TS results, we found that both trends in the observed temperature series were positive and had similar magnitudes (0.0150 and 0.0141 °C.year⁻¹ for Campinas and Piracicaba, respectively), confirming, as expected, a warmer scenario with growing temperatures.

Table 2

Classification of the 5 best copula functions for the Piracicaba and Campinas stations, based on their performances in the ML, BIC, and AIC criteria.

Station	Rank	ML	AIC	BIC	Selected copula
Piracicaba	1	BB1	BB1	BB1	BB1
	2	Tawn	t	t	
	3	t	Gaussian	Gaussian	
	4	Gaussian	Tawn	Tawn	
	5	Roch-Alegre	Roch-Alegre	Roch-Alegre	
Campinas	1	BB1	Clayton	Clayton	Clayton
	2	Clayton	BB1	BB1	
	3	Tawn	Raftery	Raftery	
	4	Raftery	Tawn	Tawn	
	5	Roch-Alegre	Roch-Alegre	Roch-Alegre	

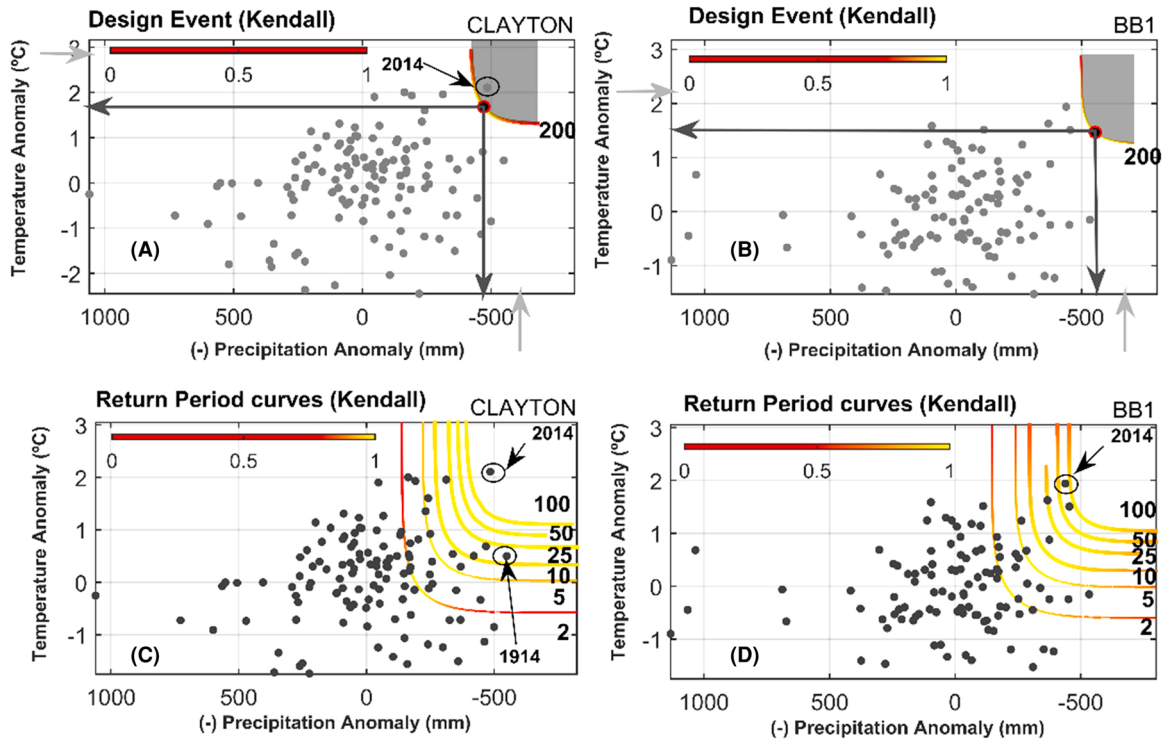


Fig. 5. The most likely design quantile (red point) associated with a 200-year return period in the multivariate framework for (A) Campinas and (B) Piracicaba. The critical region, in which the events have a higher return period, is highlighted in gray. Light gray arrows show the univariate design quantiles for a 200-year return period and dark gray arrows are the quantiles of temperature and precipitation associated with the most likely design quantile. Joint probability isolines associated with 2, 5, 10, 25, 50, and 100 year- return period for (C) Campinas and (D) Piracicaba. Isolines were colored according to their level of joint density level in yellow and red representing highest and lowest levels, respectively. The most likely quantile is associated with the highest density level. (For interpretation of the references to color in this figure legend, the reader is referred to the web version of this article.)

The positive trends found in the observed temperature series remained in future periods with a magnitude intensification in RCP4.5 (0.0236 and 0.0193 °C.year⁻¹ for Campinas and Piracicaba, respectively) and RCP8.5 (0.0710 and 0.0655 °C.year⁻¹). These findings confirm the warmer climate expected at the end of the century, which can lead to extreme drought events, and causes significant stress on the ecosystem (AghaKouchak et al., 2014). Furthermore, although no significant trends were found in the observed and future precipitation series, drought events may become more frequent and severe due to the increase in temperature observed over the last decade (Perkins et al., 2012; Vicente-Serrano et al., 2014).

3.3. Return period

3.3.1. Observed data

For each station and drought variable (temperature or precipitation), the best probability distribution was selected (Table 1) based on its performance on the evaluated goodness-of-fit criteria. Among all evaluated distributions, GEV and GLO appeared as the most

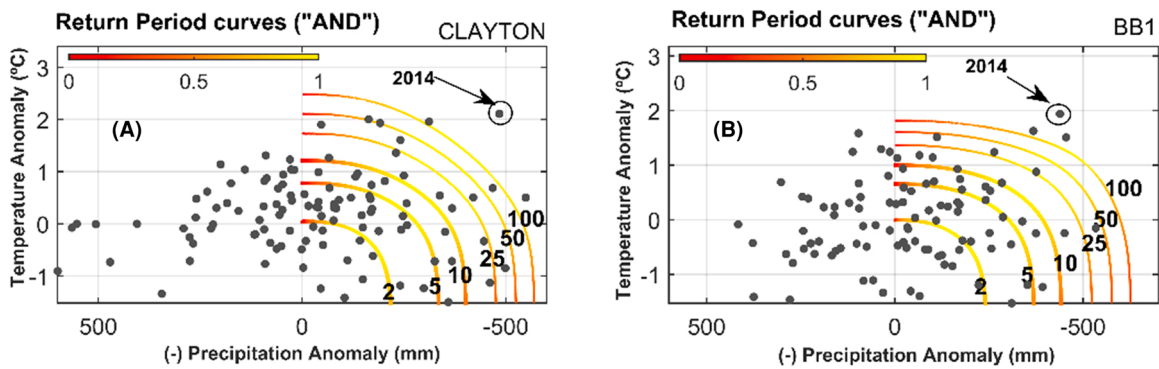


Fig. 6. Joint probability isolines of the “AND” scenario associated with 2, 5, 10, 25, 50, and 100 year-return period for (A) Campinas and (B) Piracicaba. Isolines were colored according to their level of joint density level in yellow and red representing highest and lowest levels, respectively. The most likely quantile is associated with the highest density level.

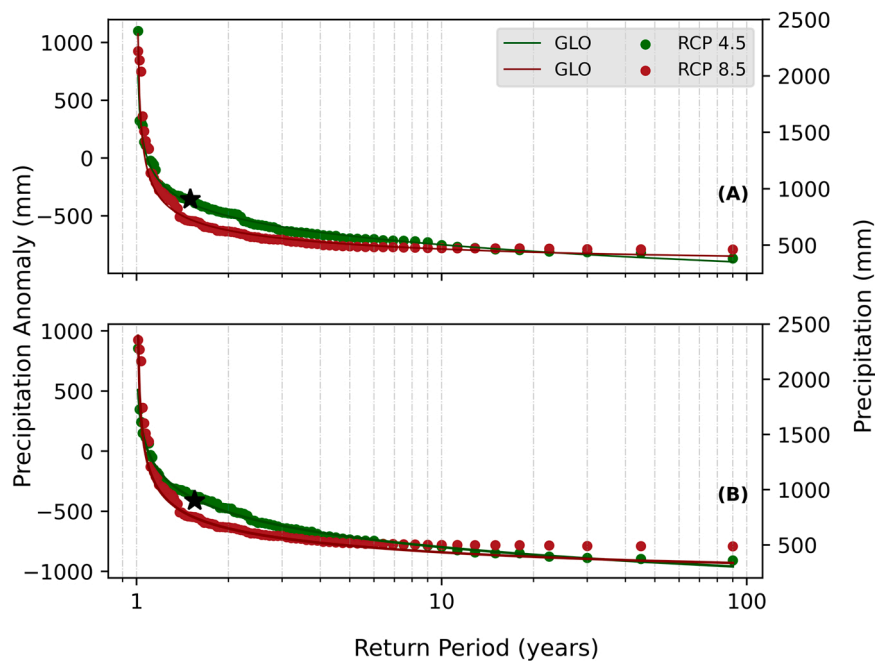


Fig. 7. Return period for both stations in the univariate framework considering future scenarios. (A) Piracicaba and (B) Campinas. The annual observed precipitation concerning the 2014–2015 drought in the study region, is shown in black. Anomalies were computed considering the mean precipitation of the observed data.

suitable distributions to represent this dataset. However, it can be seen in the Q-Q plots that all evaluated probability distributions describe the observed values similarly (Fig. S1).

Considering only precipitation data from a univariate perspective (Fig. 4), the return period of the 2014–2015 drought in the study region was approximately 25 years for Campinas and 40 years for Piracicaba. If we consider temperature data, the return period changed to approximately 100 years (Piracicaba) and 120 years (Campinas). That is, in both evaluated stations, the 2014–2015 southeast drought was not seen as an extreme and rare condition according to the common practice of using only precipitation data, despite its severe economic and social impacts. However, drought events can depend on different meteorological variables, which, when combined simultaneously, generate an extreme condition with significant impacts.

To assess the 2014–2015 water crisis according to a multivariate perspective, we used the copula framework considering drought events as a combination of extreme conditions of low precipitation and high temperature. To do this, we used the MvCAT toolbox (Sadeh et al., 2017) to select the best copula function. For both stations, the best copula functions (BB1 and Clayton, for Piracicaba and Campinas, respectively) were selected based on their performance in AIC and BIC (Table 2). It is important to note the agreement between the choices of the statistical tests. The BB1, Tawn and Roch-Alegre copulas performed well for both stations. The selected copula also showed a good performance on RMSE and NSE tests (0.1054 and 0.9980 for Piracicaba and 0.1637 and 0.9957 for

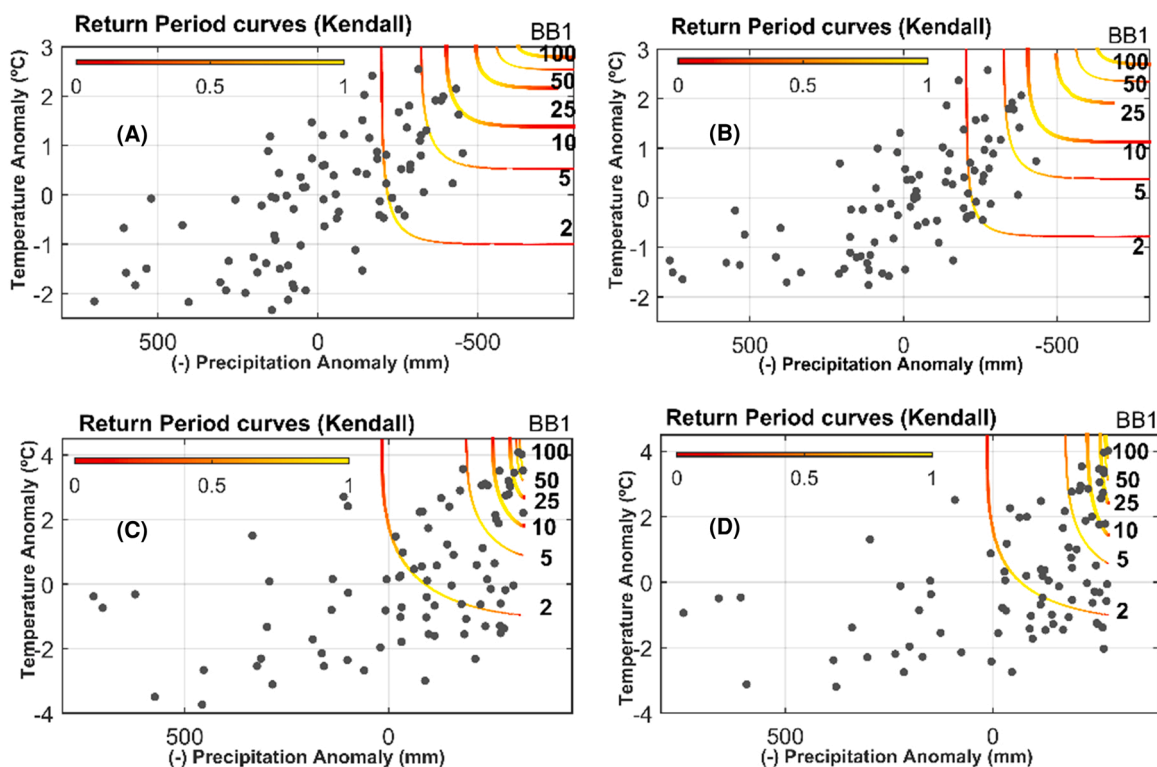


Fig. 8. Joint probability isolines associated with 2, 5, 10, 25, 50, and a 100-year return period for Campinas considering RCP4.5 (A) and RCP8.5 (C) scenarios. The same for Piracicaba, where RCP4.5 and RCP8.5 are represented in (B) and (D), respectively. Isolines are colored with joint density levels, in which yellow and red represent the highest and lowest levels, respectively. The most likely quantile is associated with the highest density level. Isolines are calculated for “Future Anomalies”. (For interpretation of the references to color in this figure legend, the reader is referred to the web version of this article.)

Campinas).

Considering the return period on the multivariate framework (Fig. 5), it can be observed that the 2014–2015 drought in the study region was classified as a rare and extreme event with a larger recurrence interval than those found in the univariate framework. In Campinas, the joint return period found is higher than 200 years whereas for Piracicaba it is approximately 80 years.

These results contrast with the univariate analysis due to the addition of the temperature variable in the frequency analysis. Drought events, as already pointed out, are the result of compound and concurrent events. Therefore, when we evaluate only a single driver, there is a possibility of misspecifications of the risks associated with extreme events. These differences (Fig. 5) highlight the importance of considering interactions between drivers for a more accurate estimation to provide a wider view of extreme events.

For both stations, various examples can be found where the univariate analysis is either underestimated or overestimated (e.g. in 1944 in Campinas, which had the lowest precipitation amount, but without an extreme temperature condition, leading to a ~20-year event from a multivariate perspective). This difference in the estimation can be attributed to the fact that the univariate framework evaluates only one driver of extreme events, ignoring all the others.

Considering a 200-year event (Fig. 5a and b) for both temperature and precipitation, the univariate approach estimates higher values than those estimated by copulas. In Piracicaba, this event is characterized by 791.27 mm (29.77 °C) annual precipitation (average daily maximum temperature), whereas in the univariate framework, the 200-year annual precipitation is 673.30 mm and the average daily maximum temperature is 30.31 °C. The same examples can be found in the “AND” scenario (Fig. 6). In this case, the differences between the univariate and the multivariate approach were even greater, given the less conservative analysis of the “AND” case (see Gräler et al. 2013).

3.3.2. Future data

The same procedure was conducted for future data to verify relative changes in the design quantiles of historical and future periods. For the univariate framework, the GLO was selected as the best probability distribution, according to the three selected goodness of fit criteria to describe the RCP4.5 and RCP8.5 simulated series. Considering the common approach (of using only precipitation data) to define design quantiles for future data, it can be observed that the return period of the reference event (2014–2015 drought in the study region) reduced to ~2 years, for all stations and plan scenarios (Fig. 7). This fact suggests that meteorological droughts will become more frequent in the future. An event classified as a 30-year event, as was characterized in the 2014–2015 studied drought considering the historical period, presented a total of ~500 mm of annual precipitation. This represents a reduction of about 40% of the total in one

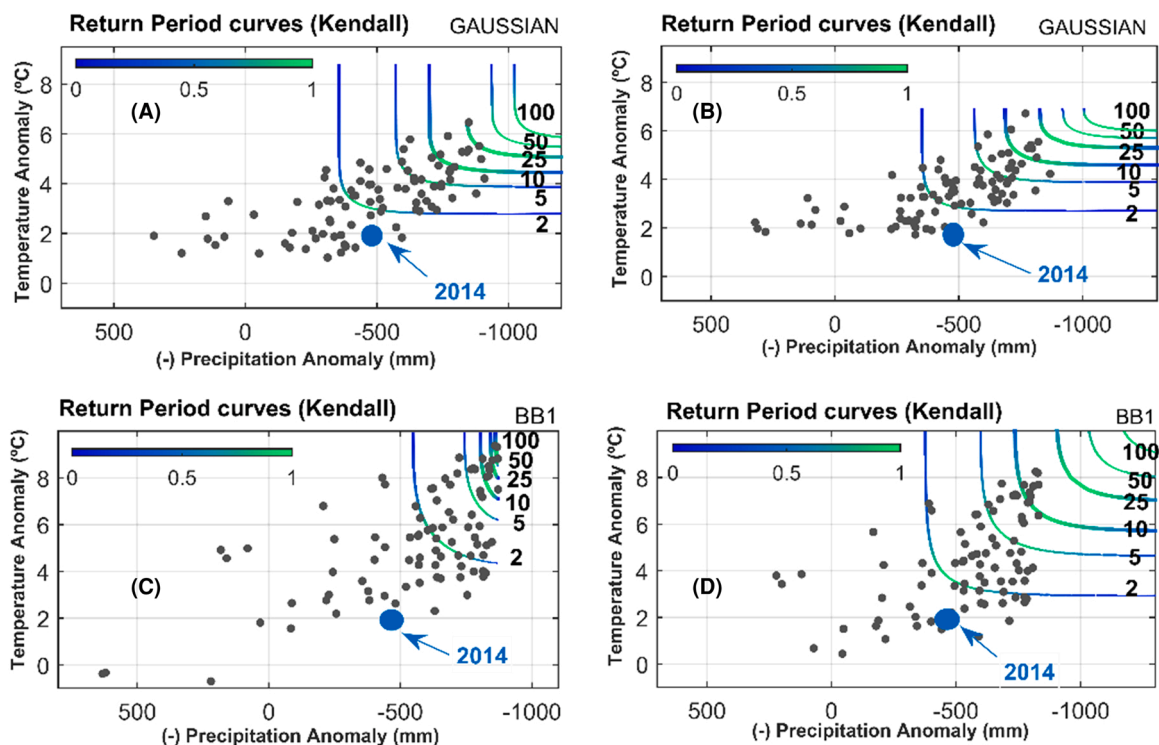


Fig. 9. Joint probability isolines associated with 2, 5, 10, 25, 50, and 100-year return period for Campinas considering the RCP4.5 (A) and RCP8.5 (C) scenarios. This is the same for Piracicaba, where RCP4.5 and RCP8.5 are represented in (C) and (D), respectively. Isolines were colored according to their level of joint density. Light blue and blue represent the highest and lowest levels, respectively. The most likely quantile is associated with the highest density level. Isolines calculated for “Present Anomalies”. (For interpretation of the references to color in this figure legend, the reader is referred to the web version of this article.)

year.

Meteorological drought characteristics were also assessed in the future period in a multivariate framework, via copulas. We focused on the Kendall’s approach in this case, as we were interested only in evaluate the changes between historical and future scenarios. However, the results can be analyzed for the “AND” case in an analogous framework.

To assess the relative changes of drought characteristics, two kinds of anomalies were considered. The first one, called “Future Anomalies”, considers deviations in the future data, calculating the anomalies as the difference between the simulated values and the mean of the future series (Fig. 8). The second methodology, called “Present Anomalies”, uses the mean of the observed data to calculate the anomalies, considering the deviations between the simulated and historical observed data (Fig. 9). Therefore, two essential aspects of droughts can be defined: their behavior and possible deviations in the future climate condition considering a warmer and drier context, and its relative changes from the current period.

In both methodologies, the BB1 copula appeared as the best function to describe meteorological drought events, as also seen in the historical period (see Tables S2 and S3 to an overall performance of the best copulas functions). Given that its formulation allows upper and lower tails dependences (Nikoloulopoulos et al., 2012), which is key property to deal with extreme events such as droughts, we suggest the BB1 copula as the most indicated function to characterize the joint occurrence of high temperature and low precipitation in the region.

According to the scenarios, extreme meteorological droughts tend to be more common (Fig. 8) when compared to historically observed ones (Fig. 5). They show a larger amplitude of climate variables with higher anomalies found in both the temperature and precipitation. This can be observed by the movement up and to the right of the isolines when compared with the isolines associated with the historical period (Fig. 5). In the present situation, an anomaly as seen in the 2014–2015 studied drought (–500 mm of annual precipitation and +2 °C average daily maximum temperature) was classified as a ~200-year return period event. In a future scenario, these anomalies are associated with a 25-year return period in both representative pathway conditions.

From the ‘present anomalies’ analysis (Fig. 9), it can be seen that drought events previously classified as extreme and rare considering the historical observed data, such as the 2014–2015 drought in the study region, were characterized as a common event, with less than 2 years of return period. This framework clarifies the expected changes in the future.

A reduction in the return period of the reference drought event (2014–2015) from ~100 to ~ less than 2 years was observed. Regarding the present climate, a 100-year future drought will be characterized as an event with approximately –900 mm precipitation anomaly and +6 °C temperature anomaly, considering the intermediate future scenario, and –1000 mm precipitation anomaly and

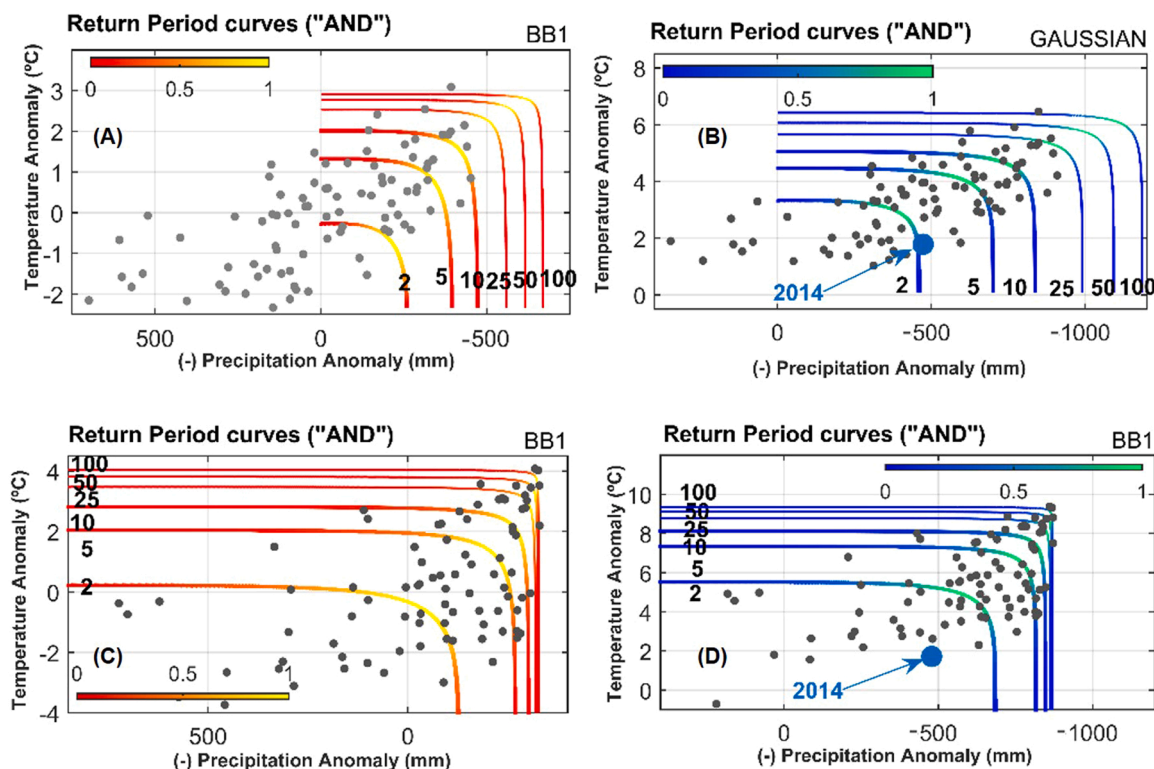


Fig. 10. Joint probability isolines associated with 2, 5, 10, 25, 50 and 100-year return period for Campinas considering RCP4.5 (top) and RCP8.5 (bottom) scenarios. Isolines were colored according to their level of joint density. Yellow and light blue represent the highest levels, while red and blue represent the lowest levels. The most likely quantile is associated with the highest density levels. Isolines were calculated for both “Future Anomalies” (left) and “Present Anomalies” (right). (For interpretation of the references to color in this figure legend, the reader is referred to the web version of this article.)

+8 °C for the pessimistic future plot. It is also important to note that in the worst scenario (RCP8.5), extreme droughts will differ, mainly due to temperature anomalies. This situation highlights the importance of considering drought as a compound event, associating temperature and precipitation, given the fact that this difference would not be noted in the univariate framework.

Similar results were found for the “AND” case. Considering the “Future Anomalies” approach for the IAC station (Fig. 10a and c), we can see that larger anomalies are expected in temperature and precipitation, for both future scenarios (RCP4.5 and RCP8.5). The reference drought was expected to be common in future conditions, being classified as a ~2-year return period and less than that for RCP4.5 and RCP8.5, respectively. In contrast to what is expected, precipitation anomalies for the RCP8.5 were smaller than those of the RCP4.5, probably due to the larger uncertainty associated with the RCP8.5 simulations. It is worth mentioning that these results represent approximate changes in meteorological dynamics. Climate model simulations are associated with a high degree of uncertainty, which affects the accuracy of these estimates.

4. Conclusion

In this study, we evaluate the differences between uni (precipitation) and multivariate (precipitation and temperature) frequency analyses to characterize extreme drought events for both present and future scenarios. The simultaneous occurrence of high temperatures and precipitation deficits may increase the socioeconomic impacts of water shortage. Evaluating the 2014–2015 southeast Brazilian water crisis, we show that the univariate approach, traditionally adopted for drought characterization, substantially underestimated the recurrence interval of this severe event. Considering that significant positive trends were found only for temperature data, we argue that the traditional approach of considering only precipitation data may lead to poor decision making in water management, especially in a climate change context. Moreover, future period analysis showed an intensification in drought characteristics. Using different perspectives (Present and Future Anomalies) helped to clarify the relative changes in drought events, indicating that (i) severe drought events, such as the 2014–2015 southeast drought, will become more common in the future and (ii) a higher occurrence of temperature and precipitation anomalies are expected. These results suggest that even if no relative changes in precipitation anomalies are expected, they are not sufficient to understand and characterize future drought events, which are also influenced by temperature anomalies.

The multivariate frequency analysis showed to be a fundamental tool for a more reliable and realistic characterization of extreme

events, which can be used for risk assessment in different applications. Agronomists can use the methodology to assist the modeling of agricultural productivity and the risk of crop failure with the occurrence of climate extremes. Water resources professionals can use it to create an operational rule to ensure water security in the face of extreme events. In essence, the use of a multivariate framework can help politicians, decision makers and the whole community in water resources management to shape public policies to deal with climate-based hazards.

For future studies, the consideration of different variables that may trigger or exacerbate drought events, such as soil moisture, water consumption, and atmospheric patterns, and the consideration of a larger set of centennial series, which are not yet available in the region, will certainly improve our knowledge and bring new insights concerning the drivers and the rarity of severe droughts.

CRediT authorship contribution statement

André S. Ballarin: Methodology, Formal analysis, Investigation, Writing – original draft, Visualization, Writing – review & editing. **Gustavo L. Barros:** Conceptualization, Methodology and Writing – original draft. **Manoel C. M. Cabrera:** Conceptualization, Writing – review & editing, Supervision. **Edson C. Wendland:** Conceptualization, Writing – review & editing, Supervision, Project administration.

Declaration of Competing Interest

The authors declare that they have no known competing financial interests or personal relationships that could have appeared to influence the work reported in this paper.

Acknowledgments

The authors acknowledge the graduate program in Hydraulics and Sanitary Engineering – PPGSHS (USP – EESC) - for the scientific support.

Funding

This work was supported by the Brazilian National Council for Scientific and Technological Development – CNPq (grant numbers 131238/2019-1; 302991/2017-4 and 140275/2012-6), by São Paulo Research Foundation – FAPESP (grant number 2015/03806-1) and by the Coordination for the Improvement of Higher Education Personnel – Brazil – CAPES (Finance code 001).

Appendix A. Supporting information

Supplementary data associated with this article can be found in the online version at [doi:10.1016/j.ejrh.2021.100970](https://doi.org/10.1016/j.ejrh.2021.100970).

References

- AghaKouchak, A., Cheng, L., Mazdiyasi, O., Farahmand, A., 2014. Global warming and changes in risk of concurrent climate extremes: insights from the 2014 California drought. *Geophys. Res. Lett.* 8847–8852. <https://doi.org/10.1002/2014GL062308>.
- Ahmad, I., Abbas, A., Saghir, A., Fawad, M., 2016. Finding probability distributions for annual daily maximum rainfall in Pakistan using linear moments and variants. *Polish J. Environ. Stud.* 25, 925–937. <https://doi.org/10.15244/pjoes/61715>.
- Almagro, A., Oliveira, P.T.S., Nearing, M.A., Hagemann, S., 2017. Projected climate change impacts in rainfall erosivity over Brazil. *Sci. Rep.* 7, 8130. <https://doi.org/10.1038/s41598-017-08298-y>.
- Almagro, A., Oliveira, P.T.S., Rosolem, R., Hagemann, S., Nobre, C.A., 2020. Performance evaluation of Eta/HadGEM2-ES and Eta/MIROC5 precipitation simulations over Brazil. *Atmos. Res.* 244, 105053. <https://doi.org/10.1016/j.atmosres.2020.105053>.
- Almazroui, M., Ashfaq, M., Islam, M.N., Rashid, I.U., Kamil, S., Abid, M.A., O'Brien, E., Ismail, M., Reboita, M.S., Sörensson, A.A., Arias, P.A., Alves, L.M., Tippett, M. K., Saeed, S., Haarsma, R., Doblaz-Reyes, F.J., Saeed, F., Kucharski, F., Nadeem, I., Silva-Vidal, Y., Rivera, J.A., Ehsan, M.A., Martínez-Castro, D., Muñoz, Á.G., Ali, M.A., Coppola, E., Sylla, M.B., 2021. Assessment of CMIP6 performance and projected temperature and precipitation changes over South America. *Earth Syst. Environ.* 5, 155–183. <https://doi.org/10.1007/s41748-021-00233-6>.
- Cannon, A.J., Sobie, S.R., Murdock, T.Q., 2015. Bias correction of GCM precipitation by quantile mapping: how well do methods preserve changes in quantiles and extremes? *J. Clim.* 28, 6938–6959. <https://doi.org/10.1175/JCLI-D-14-00754.1>.
- Chagas, V.B.P., Chaffe, P.L.B., 2018. The role of land cover in the propagation of rainfall into streamflow trends. *Water Resour. Res.* 54, 5986–6004. <https://doi.org/10.1029/2018WR022947>.
- Chou, S.C., Lyra, A., Mourão, C., Dereczynski, C., Pilotto, I., Gomes, J., Bustamante, J., Tavares, P., Silva, A., Rodrigues, D., Campos, D., Chagas, D., Sueiro, G., Siqueira, G., Marengo, J., 2014a. Assessment of climate change over South America under RCP 4.5 and 8.5 downscaling scenarios. *Am. J. Clim. Change* 03, 512–527. <https://doi.org/10.4236/ajcc.2014.35043>.
- Chou, S.C., Lyra, A., Mourão, C., Dereczynski, C., Pilotto, I., Gomes, J., Bustamante, J., Tavares, P., Silva, A., Rodrigues, D., Campos, D., Chagas, D., Sueiro, G., Siqueira, G., Nobre, P., Marengo, J., 2014b. Evaluation of the eta simulations nested in three global climate models. *Am. J. Clim. Change* 03, 438–454. <https://doi.org/10.4236/ajcc.2014.35039>.
- Coelho, C.A.S., Cardoso, D.H.F., Firpo, M.A.F., 2016a. Precipitation diagnostics of an exceptionally dry event in São Paulo, Brazil. *Theor. Appl. Climatol.* 125, 769–784. <https://doi.org/10.1007/s00704-015-1540-9>.
- Coelho, C.A.S., de Oliveira, C.P., Ambrizzi, T., Reboita, M.S., Carpenedo, C.B., Campos, J.L.P.S., Tomaziello, A.C.N., Pampuch, L.A., Custódio, M., de S., Dutra, L.M. M., Da Rocha, R.P., Rehbein, A., 2016b. The 2014 southeast Brazil austral summer drought: regional scale mechanisms and teleconnections. *Clim. Dyn.* 46, 3737–3752. <https://doi.org/10.1007/s00382-015-2800-1>.

- Coelho, C.A.S., Uvo, C.B., Ambrizzi, T., 2002. Exploring the impacts of the tropical Pacific SST on the precipitation patterns over South America during ENSO periods. *Theor. Appl. Climatol.* 71, 185–197. <https://doi.org/10.1007/s007040200004>.
- Dufek, A.S., Ambrizzi, T., 2008. Precipitation variability in São Paulo State, Brazil. *Theor. Appl. Climatol.* 93, 167–178. <https://doi.org/10.1007/s00704-007-0348-7>.
- Filho, J.D.P., Filho, F.A.S., Martins, E.S.P.R., Studart, T.M.C., 2020. Copula-based multivariate frequency analysis of the 2012–2018 drought in Northeast Brazil. *Water* 12 (3), 834. <https://doi.org/10.3390/w12030834>.
- Fischer, E.M., Knutti, R., 2013. Robust projections of combined humidity and temperature extremes. *Nat. Clim. Change* 3, 126–130. <https://doi.org/10.1038/nclimate1682>.
- Getirana, A., 2016. Extreme water deficit in Brazil detected from space. *J. Hydrometeorol.* 17, 591–599. <https://doi.org/10.1175/JHM-D-15-0096.1>.
- Gräler, B., Van Den Berg, M.J., Vandenbergh, S., Petroselli, A., Grimaldi, S., De Baets, B., Verhoest, N.E.C., 2013. Multivariate return periods in hydrology: a critical and practical review focusing on synthetic design hydrograph estimation. *Hydrol. Earth Syst. Sci.* 17, 1281–1296. <https://doi.org/10.5194/hess-17-1281-2013>.
- Gupta, H.V., Kling, H., Yilmaz, K.K., Martinez, G.F., 2009. Decomposition of the mean squared error and NSE performance criteria: implications for improving hydrological modelling. *J. Hydrol.* 377, 80–91. <https://doi.org/10.1016/j.jhydrol.2009.08.003>.
- Hamed, K.A., Rao, A.R., 1998. A modified Mann-Kendall trend test for autocorrelated data. *J. Hydrol.* 204, 182–196.
- Hao, Z., AghaKouchak, A., Nakhjiri, N., Farahmand, A., 2014. Global integrated drought monitoring and prediction system. *Sci. data* 1, 140001. <https://doi.org/10.1038/sdata.2014.1>.
- Hao, Z., Singh, V.P., Hao, F., 2018. Compound extremes in hydroclimatology: a review. *Water* 10, 16–21. <https://doi.org/10.3390/w10060718>.
- Hosking, J.R.M., 1990. L-Moments: analysis and estimation of distributions using linear combination of order statistics. *J. R. Stat. Soc.* 52, 105–124. <https://doi.org/10.1111/j.2517-6161.1990.tb01775.x>.
- Jackson, E.K., Roberts, W., Nelsen, B., Williams, G.P., Nelson, E.J., Ames, D.P., 2019. Introductory overview: error metrics for hydrologic modelling – a review of common practices and an open source library to facilitate use and adoption. *Environ. Model. Softw.* 119, 32–48. <https://doi.org/10.1016/j.envsoft.2019.05.001>.
- Kane, R.P., 2000. Relationship between El Niño timings and rainfall extremes in Ne Brazil, São Paulo city and South Brazil. *Rev. Bras. Meteorol.* 15, 45–57.
- Kao, S.C., Govindaraju, R.S., 2010. A copula-based joint deficit index for droughts. *J. Hydrol.* 380, 121–134. <https://doi.org/10.1016/j.jhydrol.2009.10.029>.
- Kao, S.C., Govindaraju, R.S., 2007. A bivariate frequency analysis of extreme rainfall with implications for design. *J. Geophys. Res. Atmos.* 112. <https://doi.org/10.1029/2007JD008522>.
- Kotlarski, S., Keuler, K., Christensen, O.B., Colette, A., Déqué, M., Gobiet, A., Goergen, K., Jacob, D., Lüthi, D., Van Meijgaard, E., Nikulin, G., Schär, C., Teichmann, C., Vautard, R., Warrach-Sagü, K., Wulfmeyer, V., 2014. Regional climate modeling on European scales: a joint standard evaluation of the EURO-CORDEX RCM ensemble. *Geosci. Model. Dev.* 7, 1297–1333. <https://doi.org/10.5194/gmd-7-1297-2014>.
- Kwon, H.-H., Lall, U., 2016. A copula-based nonstationary frequency analysis for the 2012–2015 drought in California. *Water Resour. Res.* 52, 5662–5675. <https://doi.org/10.1002/2016WR018959>.
- Leonard, M., Westra, S., Phatak, A., Lambert, M., van den Hurk, B., McInnes, K., Risbey, J., Schuster, S., Jakob, D., Stafford-Smith, M., 2014. A compound event framework for understanding extreme impacts. *WIREs Clim. Change* 5, 113–128. <https://doi.org/10.1002/wcc.252>.
- Liang, X.Z., Kunkel, K.E., Meehl, G.A., Jones, R.G., Wang, J.X.L., 2008. Regional climate models downscaling analysis of general circulation models present climate biases propagation into future change projections. *Geophys. Res. Lett.* 35, 1–5. <https://doi.org/10.1029/2007GL032849>.
- Lyra, A., Tavares, P., Chou, S.C., Sueiro, G., Dereczynski, C., Sondermann, M., Silva, A., Marengo, J., Giarolla, A., 2018. Climate change projections over three metropolitan regions in Southeast Brazil using the non-hydrostatic Eta regional climate model at 5-km resolution. *Theor. Appl. Climatol.* 132, 663–682. <https://doi.org/10.1007/s00704-017-2067-z>.
- Marengo, J.A., Alves, L.M., Alvares, R.C.S., Cunha, A.P., Brito, S., Moraes, O.L.L., 2018. Climatic characteristics of the 2010–2016 drought in the semiarid northeast Brazil region. *Ann. Braz. Acad. Sci.* 90, 1973–1985. <https://doi.org/10.1590/0001-3765201720170206>.
- Masud, M.B., Khaliq, M.N., Wheeler, H.S., 2015. Analysis of meteorological droughts for the Saskatchewan River Basin using univariate and bivariate approaches. *J. Hydrol.* 522, 452–466. <https://doi.org/10.1016/j.jhydrol.2014.12.058>.
- Mechler, R., Bouwer, L.M., 2015. Understanding trends and projections of disaster losses and climate change: is vulnerability the missing link? *Clim. Change* 133, 23–35. <https://doi.org/10.1007/s10584-014-1141-0>.
- Melo, D.C.D., Wendland, E., 2017. Shallow aquifer response to climate change scenarios in a small catchment in the guarani aquifer outcrop zone. *An. Acad. Bras. Cienc.* 89, 391–406. <https://doi.org/10.1590/0001-3765201720160264>.
- Melo, D.C.D., Wendland, E., 2016. Hydrological system time lag responses to meteorological shifts. *Rev. Bras. Recur. Hidr.* 21, 766–776. <https://doi.org/10.1590/2318-0331.011616083>.
- Melo, D.C.D., Scanlon, B.R., Zhang, Z., Wendland, E., Yin, L., 2016. Reservoir storage and hydrologic responses to droughts in the Paraná River basin, south-eastern Brazil. *Hydrol. Earth Syst. Sci.* 20, 4673–4688. <https://doi.org/10.5194/hess-20-4673-2016>.
- Mesbahzadeh, T., Mirakbari, M., Mohseni Saravi, M., Soleimani Sardoo, F., Miglietta, M.M., 2020. Meteorological drought analysis using copula theory and drought indicators under climate change scenarios (RCP). *Meteorol. Appl.* 27, e1856. <https://doi.org/10.1002/met.1856>.
- Nash, J.E., Sutcliffe, J.V., 1970. River flow forecasting through conceptual models part I - a discussion of principles. *J. Hydrol.* 10, 282–290. [https://doi.org/10.1016/0022-1694\(70\)90255-6](https://doi.org/10.1016/0022-1694(70)90255-6).
- Nikoloulopoulos, A.K., Joe, H., Li, H., 2012. Vine copulas with asymmetric tail dependence and applications to financial return data. *Comput. Stat. Data Anal.* 56, 3659–3673. <https://doi.org/10.1016/j.csda.2010.07.016>.
- Nobre, C.A., Marengo, J.A., Seluchi, M.E., Cuartas, L.A., Alves, L.M., 2016. Some characteristics and impacts of the drought and water crisis in Southeastern Brazil during 2014 and 2015. *J. Water Resour. Prot. Obs.* 8, 252–262. <https://doi.org/10.4236/jwarp.2016.82022>.
- Obregón, G.O., Marengo, J.A., Nobre, C.A., 2014. Rainfall and climate variability: long-term trends in the metropolitan area of São Paulo in the 20th century. *Clim. Res.* 61, 93–107. <https://doi.org/10.3354/cr01241>.
- Otto, F.E.L., Coelho, C.A.S., King, A.D., de Perez, E.C., Wada, Y., Van Oldenborgh, G.J., Haarsma, R., Haustein, K., Uhe, P., Van Aalst, M., Aravequia, J.A., Almeida, W., Cullen, H., 2015. Explaining Extreme Events of 2014. *Bull. Am. Meteorol. Soc.* 96, 35–40.
- Pendergrass, A.G., Meehl, G.A., Pulwarty, R., Hobbins, M., Hoell, A., AghaKouchak, A., Bonfils, C.J.W., Gallant, A.J.E., Hoerling, M., Hoffmann, D., Kaatz, L., Lehner, F., Llewellyn, D., Mote, P., Neale, R.B., Overpeck, J.T., Sheffield, A., Stahl, K., Svoboda, M., Wheeler, M.C., Wood, A.W., Woodhouse, C.A., 2020. Flash droughts present a new challenge for subseasonal-to-seasonal prediction. *Nat. Clim. Change* 10, 191–199. <https://doi.org/10.1038/s41558-020-0709-0>.
- Perkins, S.E., Alexander, L.V., Nairn, J.R., 2012. Increasing frequency, intensity and duration of observed global heatwaves and warm spells. *Geophys. Res. Lett.* 39, 1–5. <https://doi.org/10.1029/2012GL053361>.
- Pulwarty, R.S., Sivakumar, M.V.K., 2014. Information systems in a changing climate: early warnings and drought risk management. *Weather Clim. Extreme* 3, 14–21. <https://doi.org/10.1016/j.wace.2014.03.005>.
- Sadegh, M., Mofakhari, H., Gupta, H.V., Ragno, E., Mazdiyasi, O., Sanders, B., Matthew, R., AghaKouchak, A., 2018. Multihazard scenarios for analysis of compound extreme events. *Geophys. Res. Lett.* 45, 5470–5480. <https://doi.org/10.1029/2018GL077317>.
- Sadegh, M., Ragno, E., AghaKouchak, A., 2017. Multivariate copula analysis toolbox (MvCAT): describing dependence and underlying uncertainty using a Bayesian framework. *Water Resour. Res.* 53, 5166–5183. <https://doi.org/10.1002/2016WR020242>.
- Salinas, J.L., Castellari, A., Viglione, A., Kohnová, S., Kjeldsen, T.R., 2014. Regional parent flood frequency distributions in Europe - Part 1: is the GEV model suitable as a pan-European parent? *Hydrol. Earth Syst. Sci.* 18, 4381–4389. <https://doi.org/10.5194/hess-18-4381-2014>.
- Salvadori, G., De Michele, C., 2004. Frequency analysis via copulas: theoretical aspects and applications to hydrological events. *Water Resour. Res.* 40, W12511. <https://doi.org/10.1029/2004WR003133>.
- Salvadori, G., De Michele, C., Durante, F., 2011. On the return period and design in a multivariate framework. *Hydrol. Earth Syst. Sci.* 15, 3293–3305. <https://doi.org/10.5194/hess-15-3293-2011>.
- Salvadori, G., Durante, F., De Michele, C., 2013. Multivariate return period calculation via survival functions. *Water Resour. Res.* 49, 2308–2311. <https://doi.org/10.1002/wrcr.20204>.

- Salvadori, G., Durante, F., De Michele, C., Bernardi, M., Petrella, L., 2016. A multivariate copula-based framework for dealing with hazard scenarios and failure probabilities. *Water Resour. Res.* 52, 3701–3721. <https://doi.org/10.1002/2015WR017225>.
- Sattari, M.T., Rezazadeh-Joudi, A., Kusiak, A., 2017. Assessment of different methods for estimation of missing data in precipitation studies. *Hydrol. Res.* 48, 1032–1044. <https://doi.org/10.2166/nh.2016.364>.
- Serinaldi, F., 2016. Can we tell more than we can know? the limits of bivariate drought analyses in the United States. *Stoch. Environ. Res. Risk Assess.* 30, 1691–1704. <https://doi.org/10.1007/s00477-015-1124-3>.
- Serinaldi, F., 2015. Dismissing return periods! *Stoch. Environ. Res. Risk Assess.* 29, 1179–1189. <https://doi.org/10.1007/s00477-014-0916-1>.
- Serinaldi, F., Bonaccorso, B., Cancelliere, A., Grimaldi, S., 2009. Probabilistic characterization of drought properties through copulas. *Phys. Chem. Earth* 34, 596–605. <https://doi.org/10.1016/j.pce.2008.09.004>.
- Seth, A., Fernandes, K., Camargo, S.J., 2015. Two summers of São Paulo drought: origins in the western tropical Pacific. *Geophys. Res. Lett.* 42, 10816–10823. <https://doi.org/10.1002/2015GL066314>.
- Sheffield, J., Wood, E.F., 2008. Projected changes in drought occurrence under future global warming from multi-model, multi-scenario, IPCC AR4 simulations. *Clim. Dyn.* 31, 79–105. <https://doi.org/10.1007/s00382-007-0340-z>.
- Sun, P., Zhang, Q., Yao, R., Wen, Q., 2019. Hydrological drought regimes of the Huai River Basin, China: Probabilistic Behavior, Causes and Implications. *Water* 11. <https://doi.org/10.3390/w11112390>.
- Trenberth, K.E., Fasullo, J.T., Shepherd, T.G., 2015. Attribution of climate extreme events. *Nat. Clim. Change* 5, 725–730. <https://doi.org/10.1038/nclimate2657>.
- Vaghefi, S.A., Keykhai, M., Jahanbakhshi, F., Sheikholeslami, J., Ahmadi, A., Yang, H., Abbaspour, K.C., 2019. The future of extreme climate in Iran. *Sci. Rep.* 9, 1464. <https://doi.org/10.1038/s41598-018-38071-8>.
- Vicente-Serrano, S.M., Lopez-Moreno, J.I., Beguería, S., Lorenzo-Lacruz, J., Sanchez-Lorenzo, A., García-Ruiz, J.M., Azorin-Molina, C., Morán-Tejeda, E., Revuelto, J., Trigo, R., Coelho, F., Espejo, F., 2014. Evidence of increasing drought severity caused by temperature rise in southern Europe. *Environ. Res. Lett.* 9. <https://doi.org/10.1088/1748-9326/9/4/044001>.
- Villarini, G., Serinaldi, F., Smith, J.A., Krajewski, W.F., 2009. On the stationarity of annual flood peaks in the continental United States during the 20th century. *Water Resour. Res.* 45, W08417. <https://doi.org/10.1029/2008WR007645>.
- Wang, K., Dickinson, R.E., Liang, S., 2012. Global atmospheric evaporative demand over land from 1973 to 2008. *J. Clim.* 25, 8353–8361. <https://doi.org/10.1175/JCLI-D-11-00492.1>.
- Wilhite, D.A., Glantz, M.H., 1985. Understanding the drought phenomenon: the role of definitions. *Water Int* 10, 111–120. <https://doi.org/10.1080/02508068508686328>.
- Yue, S., Hashino, M., 2007. Probability distribution of annual, seasonal and monthly precipitation in Japan. *Hydrol. Sci. J.* 52, 863–877. <https://doi.org/10.1623/hysj.52.5.863>.
- Zscheischler, J., Seneviratne, S.I., 2017. Dependence of drivers affects risks associated with compound events. *Sci. Adv.* 3, 1–11. <https://doi.org/10.1126/sciadv.1700263>.